An Interlocked Figure-of-Eight Molecular Shuttle

Maxime Gauthier, Karine Fournel-Marotte, Caroline Clavel, Philip Waelès, Philippe Laurent, Frédéric Coutrot

How to cite: *Angew. Chem. Int. Ed.* **2023**, *62*, e202310643
doi.org/10.1002/anie.202310643

Supramolecular Chemistry

An Interlocked Figure-of-Eight Molecular Shuttle

*Maxime Gauthier, Karine Fournel-Marotte, Caroline Clavel, Philip Waelès, Philippe Laurent, and Frédéric Coutrot**

Abstract: Here is reported the synthesis and characterization of an interlocked figure-of-eight rotaxane molecular shuttle from a dibenzo-24-crown-8 (DB24C8) derivative. This latter bears two molecular chains, whose extremities are able to react together by click chemistry. One of the two substituting chain holds an ammonium function aimed at driving the self-entanglement through the complexation of the DB24C8 moiety. In the targeted figure-of-eight rotaxane, shuttling of the DB24C8 along the threaded axle from the best ammonium station to the weaker binding site triazolium was performed through deprotonation or deprotonation-then-carbamoylation of the ammonium. This way, two discrete *co*-conformational states were obtained, in which the folding and size of the two loops could be changed.

In the past decades, advances in supramolecular chemistry,[1] then utilization of the template effect[2] opened an avenue for the synthesis of a wide range of mechanically interlocked molecules (MIMs),[3] from catenanes[4] to rotaxanes[5] through sophisticated interlocked architectures such as interlocked linear,[6] cyclic[7] or multidimensional[8] molecular muscles, foldarotaxanes,[9] links,[10] or knots.[11] The [1]rotaxane architecture (Figure 1a),[12] whose encircled thread and surrounding macrocycle are linked together through covalent bond, may be encountered in natural compounds such as lasso peptides[13] for example. To date, this molecular architecture has been less exploited than [2]rotaxanes (Figure 1b), in which no covalent bond exists between the two embedded units. Even scarcer are the published reports about rotaxanes in which the two extremities of the encircled thread are linked to the surrounding macrocycle. Such a double connection between thread and macrocycle affords a singular [1]rotaxane molecular architecture, called a figure-of-eight (Fo8) rotaxane because it is reminiscent of that of a eight number. The first figure-of-eight rotaxane was synthesized by Vögtle et al. in 2001 through the post-synthetic conversion of a [2]rotaxane.[14] Since then, only two other examples were reported independently by Sauvage, Stoddart et al.,[15] as a methodological synthetic access, then very recently by Smith et al.[16] for the conception of novel globular and efficient fluorescent probes of high stability against enzymes and not prone to self-aggregation. Noteworthy, no Fo8 rotaxane has been synthesized to date with the aim of behaving as a molecular machine. The possibility to shuttle the macrocycle in a Fo8 rotaxane gives the opportunity to expand and contract the respective loops of the interlocked molecule.[6–8] In this paper, we report on the synthesis and characterization of a new Fo8 rotaxane molecular shuttle that consists in the combination of a DB24C8 derivative surrounding a molecular axle that contains an ammonium and a triazolium molecular stations. Unlike the preceding reported chemical pathways to Fo8 (Figure 1c), the strategy employed here consisted in synthesizing first a hermaphrodite[12d,17] molecule—i.e. a molecule containing the two complementary interacting sites that may bind together—able to self-entangle before the architecture was mechanically locked through connecting the free encircled axle extremity to the surrounding macrocycle (Figure 1d).

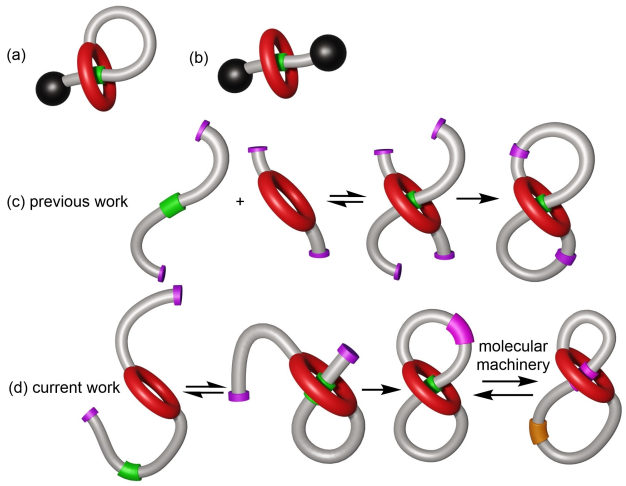

Figure 1. Representation of: (a) a [1]rotaxane; (b) a [2]rotaxane ; (c) already reported strategy to yield a Fo8 rotaxane; (d) present strategy to yield a Fo8 rotaxane molecular shuttle.

The targeted Fo8 rotaxane **3-HPF$_6$** contained an ammonium station[18] as the best pH-responsive site of interaction for the DB24C8 derivative and a *N*-meth-

[*] Dr. M. Gauthier, Dr. K. Fournel-Marotte, Dr. C. Clavel, Dr. P. Waelès, Dr. P. Laurent, Dr. F. Coutrot
Supramolecular Machines and Architectures Team, IBMM, Univ Montpellier, CNRS, ENSCM, Montpellier (France)
E-mail: frederic.coutrot@umontpellier.fr
Homepage: www.glycorotaxane.com

yltriazolium[19] as the weaker secondary station (Scheme 1). It was prepared from the *cis* disubstituted DB24C8 **1u-Boc**[20] according to a three-step sequence. Boc removal revealed the ammonium moiety on one substituting chain of the DB24C8. In the non-competitive solvent CD_2Cl_2, the hermaphrodite compound **1u-HPF$_6$** self-entangled to yield the pseudorotaxane **1-HPF$_6$** as a racemic mixture.[21] ^{1}H NMR spectrum of Figure 2a indicates the uncomplexed architecture of **1u-HPF$_6$** in the dissociating solvent DMSO because solvation of the ammonium moiety by the solvent molecules predominates over intramolecular hydrogen bonds. On contrary, evidences of the pseudorotaxane architecture **1-HPF$_6$** are noticed in the non-competitive solvent CD_2Cl_2 (Figure 2b). By comparing the two ^{1}H NMR spectra, the methylenic hydrogen atoms of the macrocyclic chain of the crown ether appear split in the pseudorotaxane **1-HPF$_6$** because they are facing the two non-symmetrical ends of the threaded axle (Figure 2b). This is not the case in the uncomplexed compound **1u-HPF$_6$** (Figure 2a). Besides, hydrogen atoms H_{19} and H_{21} that belong to the ammonium template are both shifted downfield in the pseudorotaxane structure because they interact through hydrogen bonding with the oxygen atoms of the crown ether moiety. The downfield shifts observed in DMSO for the hydrogen atoms of the amide motifs $H_{2,31,34}$ and H_{13} are unsurprisingly due to their solvation by the very polar competitive solvent. Mean-

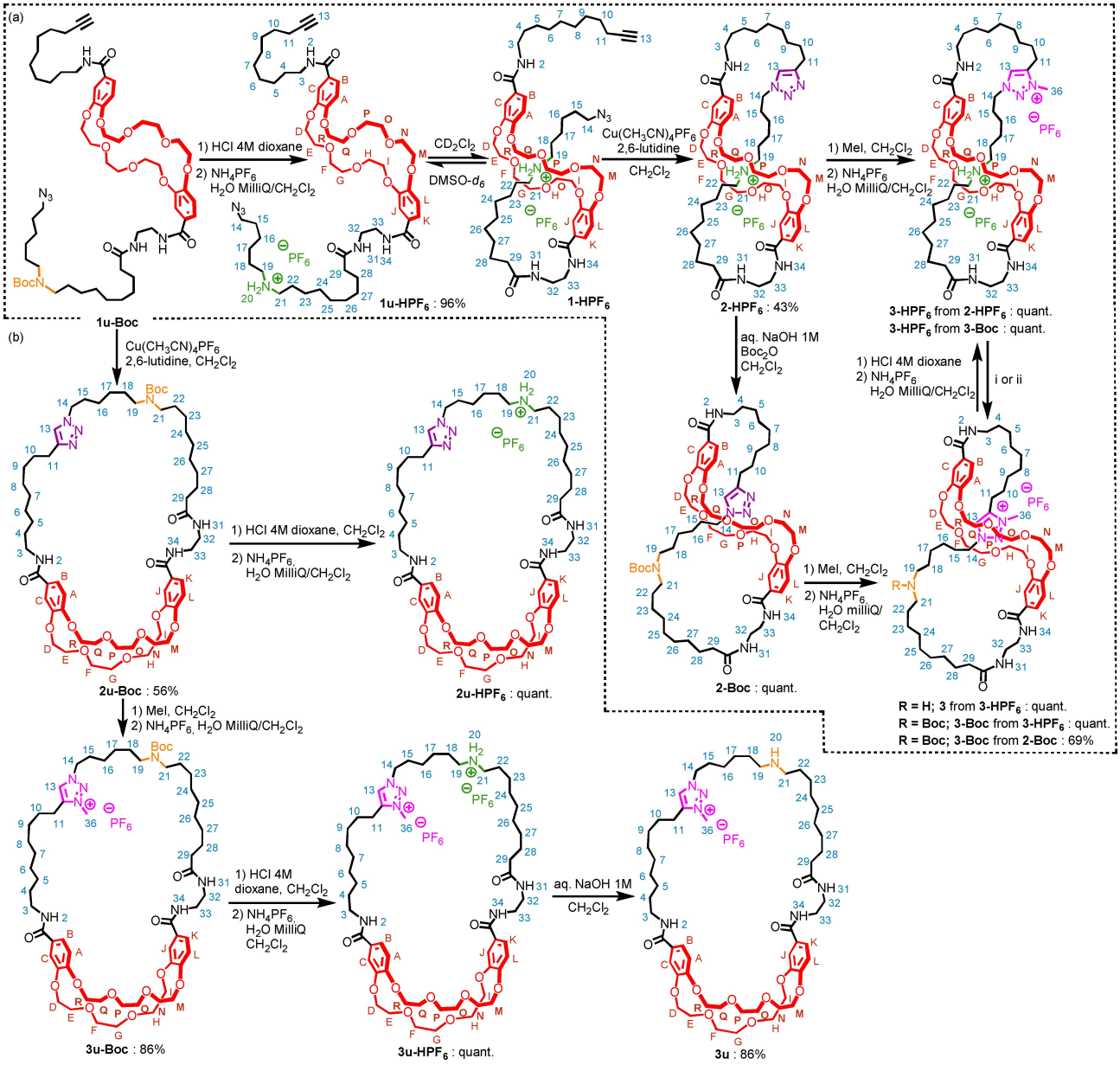

Scheme 1. (a) Synthesis of the targeted Fo8 rotaxane molecular shuttle via the hermaphrodite compound **1u-HPF$_6$**. Experimental conditions to yield compound **3**, i: BEMP resin, CD_3CN. To yield compound **3-Boc**, ii: Et_3N, Boc_2O, CD_3CN. For clarity, only one of the two enantiomers for the Fo8 rotaxanes is represented; (b) Synthesis of the non-interlocked macrobicyclic analogues from the disubstituted DB24C8 derivative **1u-Boc**.

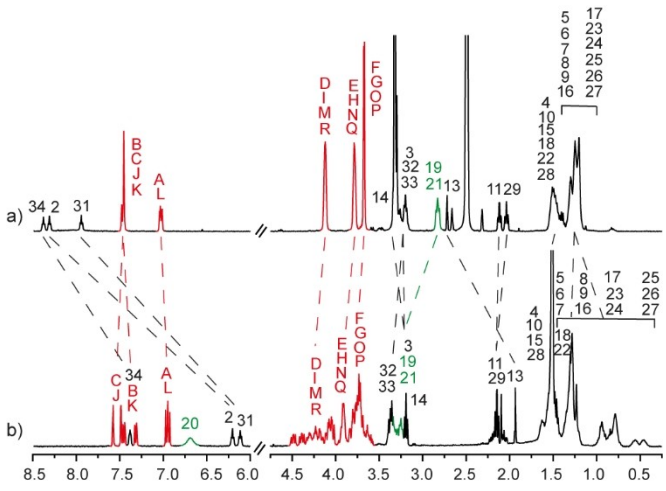

Figure 2. ^{1}H NMR spectra (400 MHz, 298 K) of the respective compounds **1u-HPF$_6$** and **1-HPF$_6$** at a concentration of 10^{-3} M in (a) DMSO-d_6 and (b) CD_2Cl_2. The numbering and lettering correspond to the proton assignments indicated in Scheme 1.

while, the same trend is observed for the much less acidic hydrogen atoms $H_{16,17}$ and $H_{23\text{-}25}$, in this case because they experience in CD_2Cl_2 the shielding effect of the aromatic rings of the crown ether. The ring-closing of pseudorotaxane **1-HPF$_6$** to yield the Fo8 rotaxane **2-HPF$_6$** was achieved in dichloromethane using the copper(I)-catalyzed Huisgen[22] alkyne-azide 1,3-dipolar cycloaddition,[23] in the presence of $Cu(CH_3CN)_4PF_6$ and 2,6-lutidine at the necessary high dilution (10^{-4} M) to avoid intermolecular side-reactions. Fo8 rotaxane **2-HPF$_6$** was isolated in a 43 % yield after purification by size exclusion chromatography using Bio-Beads S-X1 Support.

Subsequent quantitative methylation of the triazole, then counter-ion exchange, led to the formation of the hexafluorophosphate *N*-methyltriazolium as the secondary molecular station for the DB24C8. The isolated figure-of-eight **3-HPF$_6$** was the object of molecular machinery through the quantitative deprotonation (or deprotonation-then-carbamoylation) of the ammonium station. In both cases, this triggered the shuttling of the crown ether along the threaded axle from the ammonium to the triazolium station, in **3** and **3-Boc**, resulting in the tightening of one of the two loops of the Fo8 rotaxane and the simultaneous loosening of the other loop.[24] The shuttling of the crown ether was invertible through protonation of **3** or removal of the Boc protection of **3-Boc** under acidic conditions.

Molecular shuttling was evidenced by the direct comparisons between the ^{1}H NMR spectra in CD_3CN of the Fo8 rotaxanes **3-HPF$_6$**, **3** and **3-Boc** with their non-interlocked analogues[25] **3u-HPF$_6$**, **3u** and **3u-Boc** (Figure 3). Comparison between the ^{1}H NMR spectrum of the Fo8 rotaxane **3-HPF$_6$** and that of its non-interlocked analogue **3u-HPF$_6$** demonstrated the interlocked architecture of the Fo8 rotaxane and showed the main localization of the crown ether around the ammonium station (Figure 3a–b). With respect to the uncomplexed macrobicycle **3u-HPF$_6$**, methylenic hydrogen atoms of the crown ether (D, I, M, R, E, H, N, Q, F, G, O, P) are split in **3-HPF$_6$** due to the dissymmetry of the encircled thread, indicating the interlocked structure of the Fo8 rotaxane. Moreover, hydrogen atoms of the ammonium station $H_{19,21}$ are shifted downfield in **3-HPF$_6$** because of their implication in hydrogen bonding interactions with the oxygen atoms of the surrounding crown ether ($\Delta\delta = +0.37$ ppm). Upfield shifts are also noticed for the hydrogen atoms of the Fo8 rotaxane that are localized in the shielding region of the aromatic rings of the crown ether, as observed for $H_{14\text{-}17}$ ($\Delta\delta$ from -0.17 to -0.26 ppm) and $H_{23\text{-}27}$ ($\Delta\delta$ from -0.15 to -0.51 ppm).

Deprotonation of the ammonium triggered the shuttling of the crown ether towards the *N*-methyltriazolium station. The new localization of the crown ether was deduced from the comparison between ^{1}H NMR spectrum of Fo8 rotaxane **3** with that of its uncomplexed analogue **3u** (Figure 3c–d). Indeed, hydrogen atoms of the *N*-methyltriazolium site $H_{13\text{-}16}$ are deshielded in the Fo8 rotaxane because of their hydrogen bonding interactions with the oxygen atoms of the surrounding crown ether moiety ($\Delta\delta = +0.25$, $+0.59$, $+0.44$ and $+0.22$ ppm, respectively). This new localization of the surrounding macrocycle was corroborated by the tremendous upfield shift for H_{36}, H_{11} and in a lesser extent H_{10} in **3** ($\Delta\delta = -0.61$, -0.93 and -0.45 ppm, respectively) because these hydrogen atoms experienced the shielding effect of the aromatic ring of the surrounding crown ether derivative.

Deprotonation-carbamoylation of **3-HPF$_6$** using triethylamine and Boc_2O in acetonitrile led to the carbamoylated Fo8 rotaxane **3-Boc**. Same trend and similar values of ^{1}H NMR chemical shift displacements were noticed for **3-Boc** with respect to **3u-Boc** (Figure 3e–f) than those noticed between **3** and **3u** (Figure 3c–d), indicating very similar conformations for Fo8 rotaxanes **3** and **3-Boc**. Compared to **3**, signals of hydrogen atoms H_{36}, H_{11} and H_{10} were shifted upfield in **3-Boc** ($\Delta\delta = -0.66$, -0.92 and -0.46 ppm, respectively), while signals of $H_{13\text{-}16}$ were shifted downfield ($\Delta\delta = +0.23$, $+0.58$, $+0.39$ and $+0.29$ ppm, respectively).

Interestingly, Fo8 rotaxane **3-Boc** was also obtained from **2-HPF$_6$** if the carbamoylation reaction was carried out prior to the *N*-methylation of the triazole. After deprotonation-then-carbamoylation of the ammonium, one could have expected that the macrocycle would interact with the amide site, as we previously reported in the literature.[26] In this case, the localization of the amide site was certainly too close to the crown ether moiety to allow such a tightened loop. Although triazole was not known to be an efficient secondary station for DB24C8 in [2]rotaxane,[27] the macrocycle had, here, no other possibility than interacting with the very poor triazole interaction site through hydrogen bonding between the oxygen atoms of the DB24C8 and $H_{13\text{-}15}$ (see Supporting Information for the ^{1}H NMR evidences of the localization of the macrocycle around the triazole site in **2-Boc**). Subsequent methylation of the triazole led to the insulation of the sole compound **3-Boc**, corroborating the *co*-conformational state determined for **2-Boc**.

Noteworthy, with respect to their non-interlocked analogues, signals of some geminal hydrogen atoms exhibited great chemical shift inequivalence in the Fo8 rotaxanes **3**, **3-Boc** and in a lesser extent in **3-HPF$_6$**. In **3-Boc**, it is on

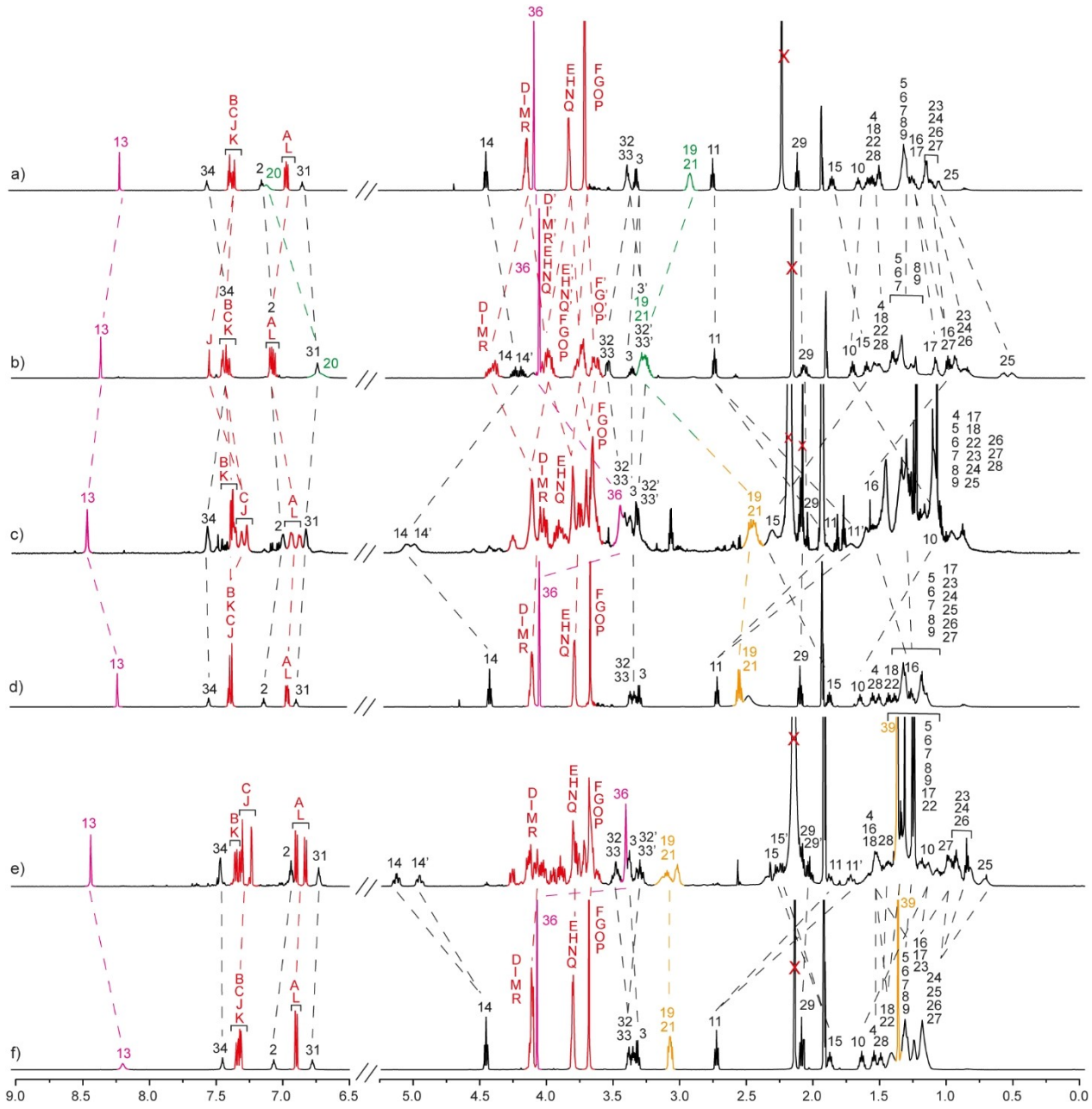

Figure 3. [1]H NMR spectra (600 MHz, CD_3CN, 298 K) of: (a) the protonated uncomplexed macrobicycle **3 u-HPF$_6$**; (b) the protonated Fo8 rotaxane **3-HPF$_6$**; (c) the deprotonated Fo8 rotaxane **3**; (d) the deprotonated uncomplexed macrobicycle **3 u**; (e) the carbamoylated Fo8 rotaxane **3-Boc**; (f) the carbamoylated uncomplexed macrobicycle**3u-Boc**. The numbering and lettering correspond to the proton assignments indicated in Scheme 1.

particularly the case of the diastereotopic methylene hydrogen atoms H_{11}, H_{14} and H_{15} being on either side of the *N*-methyltriazolium ($\Delta\delta = +0.16$, $+0.17$ and $+0.08$ ppm for the difference of chemical shift between the respective pairs of geminal hydrogen atoms H_{11}-$H_{11'}$, H_{14}-$H_{14'}$ and H_{15}-$H_{15'}$, respectively in **3-Boc**). This was also observed for hydrogen atoms H_{32}, H_{33} and in a lesser extent H_{29}, all belonging to the peripheral of one of the two loops of the Fo8 rotaxane ($\Delta\delta = +0.21$, $+0.15$ and $+0.07$ ppm for the difference of chemical shift between the respective pairs of geminal hydrogen atoms H_{32}-$H_{32'}$, H_{33}-$H_{33'}$ and H_{29}-$H_{29'}$, respectively in **3-Boc**). This greater differentiation of geminal hydrogen atoms provided evidence of conformational restriction for the Fo8 rotaxanes with respect to non-interlocked analogues. In **3-HPF$_6$**, this difference of chemical shift between geminal hydrogen atoms was more pronounced for the respective pairs H_{32}-$H_{32'}$ and H_{33}-$H_{33'}$ ($\Delta\delta = +0.26$ ppm for both), highlighting the lower conformational degree of freedom of the tightened loop containing $H_{32\text{-}33}$—i.e. when the crown ether lied around the ammonium station. However, with respect to **3-Boc** much less differences of chemical shift between geminal hydrogen atoms H_{11}, $H_{14\text{-}15}$ were noticed, corroborating the higher degree of freedom of the loosened loop that contained these atoms.[28]

In conclusion, we reported herein the first Fo8 rotaxane able to act as a molecular shuttle. With respect to linear analogues, cyclic molecules are known for their singular properties that are related to their restrained conformational degree of freedom. In parallel, interlocked rotaxane molecular machines gained interest in the past decades because of their peculiar switchable physical and chemical properties. Combining both structural properties in cyclic interlocked molecular machines such as the very aesthetic Fo8 rotaxane molecular architecture allowed for interdependent tightening or loosening motion of the two loops of the single molecule. With such a molecular architecture, taking advantage of this invertible motion might confer dual responsive property to the molecule.

Conflict of Interest

The authors declare no conflict of interest.

Data Availability Statement

The data that support the findings of this study are available in the supplementary material of this article.

Keywords: Dibenzo-24-Crown-8 · Figure of 8 · Mechanical Bond · Molecular Shuttle · Rotaxane

[1] The term "supramolecular" was introduced for the first time in 1978, see: J.-M. Lehn, *Pure Appl. Chem.* **1978**, *50*, 871–892. J.-M. Lehn shared the Nobel Prize in Chemistry in 1987 with D. J. Cram and C. Pedersen.

[2] C. O. Dietrich-Buchecker, J.-P. Sauvage, J.-P. Kintzinger, *Tetrahedron Lett.* **1983**, *24*, 5095–5098.

[3] a) C. Bruns, J. F. Stoddart, *The Nature of the Mechanical Bond: From Molecules to Machines*, Wiley, Hoboken, **2017**; b) S. F. M. van Dongen, S. Cantekin, J. A. A. W. Elemans, A. E. Rowan, R. J. M. Nolte, *Chem. Soc. Rev.* **2014**, *43*, 99–122; c) A. H. G. David, J. F. Stoddart, *Isr. J. Chem.* **2021**, *61*, 608–621; d) P. Waelès, M. Gauthier, F. Coutrot, *Angew. Chem. Int. Ed.* **2021**, *60*, 16778–16799; e) M. Gauthier, P. Waelès, F. Coutrot, *ChemPlusChem* **2022**, *87*, e20210045; f) D. Sluysmans, J. F. Stoddart, *Trends Chem.* **2019**, *1*, 185–197; g) B. Taghavi Shahraki, S. Maghsoudi, Y. Fatahi, N. Rabiee, S. Bahadorikhalili, R. Dinarvand, M. Bagherzadeh, F. Verpoort, *Coord. Chem. Rev.* **2020**, *423*, 213484; h) M. S. Vickers, P. D. Beer, *Chem. Soc. Rev.* **2007**, *36*, 211–225; i) L. Fang, M. A. Olson, D. Benitez, E. Tkatchouk, W. A. Goddard, J. F. Stoddart, *Chem. Soc. Rev.* **2010**, *39*, 17–29; j) J. E. Beves, B. A. Blight, C. J. Campbell, D. A. Leigh, R. T. McBurney, *Angew. Chem. Int. Ed.* **2011**, *50*, 9260–9327.

[4] a) G. Gil-Ramírez, D. A. Leigh, A. J. Stephens, *Angew. Chem. Int. Ed.* **2015**, *54*, 6110–6150; b) N. H. Evans, P. D. Beer, *Chem. Soc. Rev.* **2014**, *43*, 4658–4683; c) H. Y. Au-Yeung, C.-C. Yee, A. W. H. Ng, K. Hu, *Inorg. Chem.* **2018**, *57*, 3475–3485.

[5] a) M. Xue, Y. Yang, X. Chi, X. Yan, F. Huang, *Chem. Rev.* **2015**, *115*, 7398–7501; b) "Functional Rotaxanes": C.-X. Zhao, Q. Zhang, G. London, D.-H. Qu in *Handbook of Macrocyclic Supramolecular Assembly* (Eds.: Y. Liu, Y. Chen, H. Y. Zhang), Springer, Singapore, **2020**, pp. 277–310; c) G. Wenz, B.-H. Han, A. Müller, *Chem. Rev.* **2006**, *106*, 782–817; d) H. Tian, Q.-C. Wang, *Chem. Soc. Rev.* **2006**, *35*, 361–374.

[6] a) M. C. Jiménez, C. Dietrich-Buchecker, J.-P. Sauvage, *Angew. Chem. Int. Ed.* **2000**, *39*, 3284–3287; b) C. Romuald, E. Busseron, F. Coutrot, *Org. Lett.* **2008**, *10*, 3741–3744; c) R. E. Dawson, S. F. Lincoln, C. J. Easton, *Chem. Commun.* **2008**, 3980–3982; d) C. Romuald, E. Busseron, F. Coutrot, *J. Org. Chem.* **2010**, *75*, 6516–6531; e) P. Waelès, B. Riss-Yaw, F. Coutrot, *Chem. Eur. J.* **2016**, *22*, 6837–6845; f) F. Niess, V. Duplan, J.-P. Sauvage, *Chem. Lett.* **2014**, *43*, 964–974; g) C. J. Bruns, J. F. Stoddart, *Acc. Chem. Res.* **2014**, *47*, 2186–2199; h) J. Rotzler, M. Mayor, *Chem. Soc. Rev.* **2013**, *42*, 44–62.

[7] a) C. Romuald, A. Ardá, C. Clavel, J. Jiménez-Barbero, F. Coutrot, *Chem. Sci.* **2012**, *3*, 1851–1857; b) S.-J. Rao, X.-H. Ye, Q. Zhang, C. Gao, W.-Z. Wang, D.-H. Qu, Asian, *J. Org. Chem.* **2018**, *7*, 902–905; c) C. Romuald, G. Cazals, C. Enjalbal, F. Coutrot, *Org. Lett.* **2013**, *15*, 184–187.

[8] a) J.-C. Chang, S.-H. Tseng, C.-C. Lai, Y.-H. Liu, S.-M. Peng, S.-H. Chiu, *Nat. Chem.* **2017**, *9*, 128–134; b) K. Fournel-Marotte, F. Coutrot, *Nat. Chem.* **2017**, *9*, 105–106.

[9] a) M. Gauthier, V. Koehler, C. Clavel, B. Kauffmann, I. Huc, Y. Ferrand, F. Coutrot, *Angew. Chem. Int. Ed.* **2021**, *60*, 8380–8384; b) V. Koehler, M. Gauthier, C. Yao, K. Fournel-Marotte, P. Waelès, B. Kauffmann, I. Huc, F. Coutrot, Y. Ferrand, *Chem. Commun.* **2022**, *58*, 8618–8621.

[10] W.-X. Gao, H.-J. Feng, B.-B. Guo, Y. Lu, G.-X. Jin, *Chem. Rev.* **2020**, *120*, 6288–6325.

[11] a) S. D. P. Fielden, D. A. Leigh, S. L. Woltering, *Angew. Chem. Int. Ed.* **2017**, *56*, 11166–11194; b) Q.-H. Guo, Y. Jiao, Y. Feng, J. F. Stoddart, *CCS Chem.* **2021**, *3*, 1542–1572; c) C. O. Dietrich-Buchecker, J.-P. Sauvage, *Angew. Chem. Int. Ed.* **1989**, *28*, 189–192; d) G. Rapenne, C. Dietrich-Buchecker, J.-P. Sauvage, *J. Am. Chem. Soc.* **1996**, *118*, 10932–10933.

[12] a) *Single Molecular Machines and Motors, Series: Advances in Atom and Single Molecule Machines* (Eds.: F. Coutrot, C. Joachim, G. Rapenne) in, Springer International Publishing Switzerland, Cham, **2015**, pp. 35–64; b) A. R. Puente, A. Bessaguet, N. Pairault, G. Pieters, J. Crassous, P. L. Polavarapu, I. Opalinski, S. Papot, *Chirality* **2021**, *33*, 773–782; c) N. Pairault, A. Bessaguet, R. Barat, L. Frédéric, G. Pieters, J. Crassous, I. Opalinski, S. Papot, *Chem. Sci.* **2021**,*12*, 2521–2526; d) C. Clavel, C. Romuald, E. Brabet, F. Coutrot, *Chem. Eur. J.* **2013**, *19*, 2982–2989; e) C. Clavel, K. Fournel-Marotte, F. Coutrot, *Molecules* **2013**, *18*, 11553–11575; f) P. Waelès, C. Clavel, K. Fournel-Marotte, F. Coutrot, *Chem. Sci.* **2015**, *6*, 4828–4836; g) H. Tian, R. Li, P.-H. Lin, K. Meguellati, *New J. Chem.* **2020**, *44*, 10628–10632; h) F. Saito, J. W. Bode, *Chem. Sci.* **2017**, *8*, 2878–2884; i) G. Orlandini, L. Casimiro, M. Bazzoni, B. Cogliati, A. Credi, M. Lucarini, S. Silvi, A. Arduini, A. Secchi, *Org. Chem. Front.* **2020**, *7*, 648–659; j) H. Li, H. Zhang, Q. Zhang, Q.-W. Zhang, D.-H. Qu, *Org. Lett.* **2012**, *14*, 5900–5903; k) K. Hiratani, M. Kaneyama, Y. Nagawa, E. Koyama, M. Kanesato, *J. Am. Chem. Soc.* **2004**, *126*, 13568–13569.

[13] a) H. Martin-Gómeza, J. Tulla-Puche, *Org. Biomol. Chem.* **2018**, *16*, 5065–5080; b) S. M. Rowe, D. R. Spring, *Chem. Soc. Rev.* **2021**, *50*, 4245–4258.

[14] C. Reuter, W. Wienand, C. Schmuck, F. Vögtle, *Chem. Eur. J.* **2001**, *7*, 1728–1733.

[15] a) M. M. Boyle, R. S. Forgan, D. C. Friedman, J. J. Gassensmith, R. A. Smaldone, J. F. Stoddart, J.-P. Sauvage, *Chem. Commun.* **2011**, *47*, 11870–11872; b) M. M. Boyle, J. J. Gassensmith, A. C. Whalley, R. S. Forgan, R. A. Smaldone, K. J. Hartlieb, A. K. Blackburn, J.-P. Sauvage, J. F. Stoddart, *Chem. Eur. J.* **2012**, *18*, 10312–10323.

[16] a) C. Zhai, C. L. Schreiber, S. Padilla-Coley, A. G. Oliver, B. D. Smith, *Angew. Chem. Int. Ed.* **2020**, *59*, 23740–23747;

b) C. L. Schreiber, C. Zhai, B. D. Smith, *Org. Biomol. Chem.* **2021**, *19*, 3213–3219; c) C. L. Schreiber, C. Zhai, B. D. Smith, *Photochem. Photobiol.* **2022**, *98*, 354–361; d) K. Kniazev, T. Guo, C. Zhai, R. S. Gamage, S. Ghonge, P. A. Frantsuzov, M. Kuno, B. D. Smith, *Dyes Pigm.* **2023**, *210*, 111031.

[17] M. Consuelo Jiménez, C. Dietrich-Buchecker, J.-P. Sauvage, A. De Cian, *Angew. Chem. Int. Ed.* **2000**, *39*, 1295–1298.

[18] A. G. Kolchinski, D. H. Busch, N. W. Alcock, *J. Chem. Soc. Chem. Commun.* **1995**, 1289–1291.

[19] F. Coutrot, *ChemistryOpen* **2015**, *4*, 556–576.

[20] The *cis* isomer was chosen for synthetic reason. Multi-step stereoselective synthesis of DB24C8 derivative **1u-Boc** is reported in the Supporting Information.

[21] Pseudorotaxane **1-HPF$_6$** and the following Fo8 rotaxanes exist as a racemic mixture of enantiomers due to the possibility for the macrocycle to be threaded via its two equivalent faces.

[22] a) R. Huisgen, *Pure Appl. Chem.* **1989**, *61*, 613–628; b) R. Huisgen, *Angew. Chem. Int. Ed. Engl.* **1963**, *2*, 565–598; c) R. Huisgen, G. Szeimies, L. Möbius, *Chem. Ber.* **1967**, *100*, 2494–2507; d) R. Huisgen, *Angew. Chem. Int. Ed. Engl.* **1963**, *2*, 633–645.

[23] a) H. C. Kolb, M. G. Finn, K. B. Sharpless, *Angew. Chem. Int. Ed.* **2001**, *40*, 2004–2021; b) C. W. Tornøe, C. Christensen, M. Meldal, *J. Org. Chem.* **2002**, *67*, 3057–3064.

[24] The estimated distance between the furthest atoms of the most enlarged loop conformations are: a) for **3-HPF6**, *ca* 13.9 Å between N_{20} and C_7; 8.5 Å between N_{20} and N_{31}; b) for **3**, *ca* 10.4 Å between C_{14} and C_4; 10.4 Å between C_{14} and C_{33}. See Supporting Information for energy minimized molecular models of **3-HPF$_6$** and **3**.

[25] See Supporting Information for details about the synthesis and characterization of all non-interlocked macrobicycles, according to scheme .

[26] B. Riss-Yaw, J. Morin, C. Clavel, F. Coutrot, *Molecules* **2017**, *22*, 2017.

[27] F. Coutrot, E. Busseron, *Chem. Eur. J.* **2008**, *14*, 4784–4787.

[28] Supplementary ^{1}H NMR ROESY experiments were carried out and corroborated the *co*-conformations of the Fo8 rotaxanes described above. Variable Temperature ^{1}H NMR experiments were also carried out and gave insights about exchanges between some hydrogen atoms (see Supporting Information).

Manuscript received: July 25, 2023
Accepted manuscript online: August 18, 2023
Version of record online: August 28, 2023